Polymer 51 (2010) 6093–6098

Contents lists available at ScienceDirect

Polymer

journal homepage: www.elsevier.com/locate/polymer

Polymer Communication

Photolithographically patterned smart hydrogel based bilayer actuators

Noy Bassik [a,b], Beza T. Abebe [c], Kate E. Laflin [a], David H. Gracias [a,d,*]

[a] Department of Chemical and Biomolecular Engineering, The Johns Hopkins University, 3400 N Charles Street, Baltimore, MD 21218, USA
[b] School of Medicine, The Johns Hopkins University, 733 N. Broadway, Baltimore, MD 21205, USA
[c] Department of Materials Science and Engineering, The Johns Hopkins University, 3400 N Charles Street, Baltimore, MD 21218, USA
[d] Department of Chemistry, The Johns Hopkins University, 3400 N Charles Street, Baltimore, MD 21218, USA

ARTICLE INFO

Article history:
Received 24 August 2010
Received in revised form
20 October 2010
Accepted 22 October 2010
Available online 28 October 2010

Keywords:
Hydrogel
Smart polymer
Actuator

ABSTRACT

We describe the fabrication of photopatterned actuators, composed of stimuli-responsive hydrogel bilayers made from N-isopropyl-acrylamide (NIPAm), acrylic acid (AAc), and poly-ethylene oxide diacrylate (PEODA). The hydrogels were deposited by spin coating and casting and were patterned by non-contact photolithography. We investigated the swelling behavior of the individual photopatterned hydrogels in aqueous solutions of varying pH and ionic strength (IS). By combining materials with optimal swelling responses, bilayer structures were triggered via changes in pH and IS to actuate into three dimensional (3D) structures. We also used these hydrogel bilayers as hinges to actuate integrated structures composed of rigid polymeric SU-8 panels, patterned to resemble the shape of a Venus Flytrap. This system provides a straightforward way to design and fabricate actuator hinges composed entirely of polymers.

1. Introduction

Photolithographic patterning is precise and enables the creation of integrated structures in a highly parallel manner [1–3]. This technique has mainly been applied to metallic and semiconductor integration, and is inherently two dimensional (2D). Thus it is challenging to generate 3D patterned structures. Chemically-responsive self-folding of 2D structures provides a mechanism to overcome these limitations and create a wide variety of complex 3D structures including chemo-mechanical actuators [4,5].

Metallic and semiconductor components have been used as precursors for self-folding of sheets, containers, and microgrippers, using either surface tension or intrinsic thin film stresses [6–8]. However, in many applications such as biological devices, there is a need to incorporate bio-friendly materials such as polymers. The incorporation of smart polymers such as hydrogels offers the possibility for stimuli-responsive structures. For example, Guan et al. [9] developed polymeric self-folding chitosan/poly(ethylene glycol methacrylate-co-ethylene glycol dimethacrylate) bilayers which fold in the presence of water. Related bilayers patterned from poly (methyacrylic acid)/poly(hydroxyethyl methacrylate) folded in solution as a result of pH-related swelling differential, and were used as a drug delivery platform in the digestive tract [10]. We sought to design an all-polymer scheme with a focus on direct patterning using photocrosslinking. We demonstrate the development of photo-patterned hydrogels composed of copolymerized N-isopropyl-acrylamide (NIPAm), Acrylic Acid (AAc), poly-hydroxyl ethyl methacrylate (HEMA), and poly-ethylene oxide diacrylate (PEODA) and their integration using photolithography. Our approach does not require plasma etching or stamping [11]; rather the polymer is directly crosslinked with UV light. This direct patterning allows for integration of bilayer actuators with rigid panels to enable the construction of complex, patterned, 3D structures that are biocompatible, economical to fabricate, and may be useful in micro tools.

NIPAm has been widely investigated for its ability to undergo fast phase transitions as a result of temperature changes. By copolymerizing NIPAm with pH-responsive monomers such as AAc, it is possible to design a dual (temperature and pH) responsive hydrogel system. It has been previously demonstrated that copolymerization of NIPAm with HEMA [12] and poly-ethylene oxide (PEO) can be used to design biodegradable biomaterials that are applicable in medical fields. The effects of ionic strength (IS) and pH on hydrodynamic diameter of NIPAm-based microgel particles have also been studied [13–16]. A decrease in hydrodynamic diameter was observed when microgels were exposed to an increase in IS. However, previous studies utilized solution-based polymerization techniques, and the results warranted an extension to photo-patterned devices. Previously, PNIPAm in an organic solvent (1-butanol) was crosslinked into specific 2D shapes to study solvent driven motion [17]. A key formulation parameter for enabling

* Corresponding author. Department of Chemical and Biomolecular Engineering, The Johns Hopkins University, 3400 N Charles Street, Baltimore, MD 21218, USA.
E-mail address: dgracias@jhu.edu (D.H. Gracias).

0032-3861/$ – see front matter © 2010 Elsevier Ltd. All rights reserved.
doi:10.1016/j.polymer.2010.10.035

photocrosslinking was the inclusion of both the NIPAm monomer and pre-polymerized chains in the precursor solution, which allowed for adequate viscosity and UV sensitivity.

We copolymerized NIPAm with AAc or HEMA via photocrosslinking to result in a pH- and IS-sensitive component of a bilayer actuator. After patterning, we tested the component hydrogel layers, namely NIPAm, NIPAm-AAc, NIPAm-HEMA, and PEODA, individually for sensitivity of swelling ratio to changes in pH and IS. This swelling data formed the basis for a hinged actuator design based on differential swelling in pH and IS. We were able to design a structure reminiscent of the Venus Flytrap (VF) plant [18] using rigid SU-8 panels and a connecting hinge. The VF opened and closed reversibly on exposure to varying pH and IS, demonstrating a straightforward fabrication technique for integration of hydrogel hinged actuators.

2. Experimental

2.1. Synthesis of photopolymerizable hydrogels

NIPAm solution was prepared by mixing of 3 g NIPAm monomer (Scientific Polymer Products Inc.), 0.4 g poly-N-isopropylacrylamide (PNIPAm, 300k molecular weight, Scientific Polymer Products Inc.) and 0.18 g BIS-Acrylamide (N,N-Methylenebis-Acrylamide) (Aldrich), dissolved in 7.5 mL of n-butanol (Sigma). The solution was vortexed overnight to aid dissolution of the PNIPAm and then decanted (after settling) to remove any insoluble crystals. One hundred microliters of photoinitiator, Irgacure 2100 (Ciba), was added to the solution just prior to photolithographic patterning. NIPAm-AAc copolymer was prepared by adding 0.31 mL Acrylic Acid (Aldrich) to the above NIPAm/PNIPAm solution after decanting.

NIPAm-HEMA solution was prepared by mixing 2 g of NIPAm monomer, 0.15 g BIS-Acrylamide, 0.920 mL hydroxylethyl methacrylate (HEMA, Scientific Polymer Products Inc.), 76 μL Ethylene Glycol Dimethacrylate (EGDMA, Scientific Polymer Products Inc.), 5 mL Carboxymethylcellulose in water (1% w/v), 1 mL water and 2.2 mL Dimethyl sulfoxide (DMSO). The solution was vortexed overnight. 2.9 mL of 30% Lucirin TPO-L (BASF)/DMSO (v/v) was added to 8.75 mL NIPAm-HEMA solution.

Polyethylene Glycol Diacrylate (7 mL), 2022 Polyethylene Glycol Diacrylate (7 mL) (PEGDA, 726 MW Scientific Polymer Products Inc.) was mixed with 10 μL Irgacure 2022 and covered with aluminum foil to protect from prepolymerization.

2.2. Photopatterning of hydrogels

Solutions were cast (to study swelling) or spun (to create integrated structures) onto a glass slide. NIPAm and NIPAm-AAc were exposed to UV light at approximately 50 mJ/cm^2 (measured at 365 nm). NIPAm-HEMA was exposed at 70 mJ/cm^2. PEODA was exposed at approximately 90 mJ/cm^2. The optimum exposure varied depending on desired sample thickness and photoinitiator concentration. NIPAm, NIPAm-AAc, and PEODA were developed in ethanol and placed in deionized (DI) water overnight before swelling analysis. The crosslinked NIPAm-HEMA structures were developed in subsequent baths of isopropanol (IPA), ethanol, and methanol. NIPAm-HEMA gels were left in methanol over night to dissolve and remove unpolymerized monomer and initiator. The methanol was replaced by DI water and the NIPAm-HEMA gels were allowed to swell for 7 h before further testing.

2.3. Preparation of bilayer structures

The photopolymerization was performed in non-contact mode, using a transparency mask (Fineline Imaging, Colorado Springs, CO) and a commercial mask aligner (Quintel). The PEODA/NIPAm-AAc bilayers were prepared by spin coating PEODA/Irgacure 2022 solution on a clean silicon wafer at 1000 rpm. After exposing at energies of approximately 50 mJ/cm^2, the NIPAm-AAc solution was cast on top and exposed for an additional 90 mJ/cm^2 as seen in Fig. 1. We observed that pure PEODA had low miscibility in butanol, and therefore the PEODA monomer solution did not mix with other layers in the photopatterning process. The polymerized patterns were developed in ethanol. The thickness of the bilayer was approximately 225 μm. Multiple VF sizes were fabricated with sizes ranging from several mm to approximately 2 cm. The photopatterned shapes were then released from the glass slide in DI water. The bending of PEODA/NIPAm-AAc bilayer system was triggered by changing the IS and pH of the solvents as shown in Fig. 2.

2.4. Preparation of hinged actuators

We also fabricated VFs composed of both rigid polymer panels and PEODA/NIPAm-AAc bilayer hinges. The rigid panels were prepared by spin coating SU-8 2015 (Microchem) at 2000 rpm on a glass slide to provide an approximately 20 μm thick film. After exposing at approximately 530 mJ/cm^2, the panels were developed for 55 s in Propylene Glycol Monomethyl Ether Acetate (PGMEA) and rinsed with IPA. Prior to bilayer coating, the slides were plasma cleaned for 2 min. Bilayers were prepared using the same method as above. Structures were released from the slide in DI water. These structures were actuated by changing the IS and pH of the solution.

2.5. Preparation of buffers

Four stock solutions of 200 mL each were prepared at pH 2.5, 4.8, 7.8, and 12.1 with an IS of 0.2M using phosphate salts. In order to study the effect of IS on the swelling of NIPAm-based gels, additional buffers were prepared by taking 50 mL from the stock and adding appropriate amounts of NaCl. It should be noted that we anticipate minimal coupling between pH and IS since we kept one value approximately constant while varying the other.

2.6. Swelling ratio analysis

To analyze swelling ratios, centimeter-sized shapes, with a thickness of 1 mm or less of each material were photocrosslinked as described above. The samples were placed in DI water for 6 h to

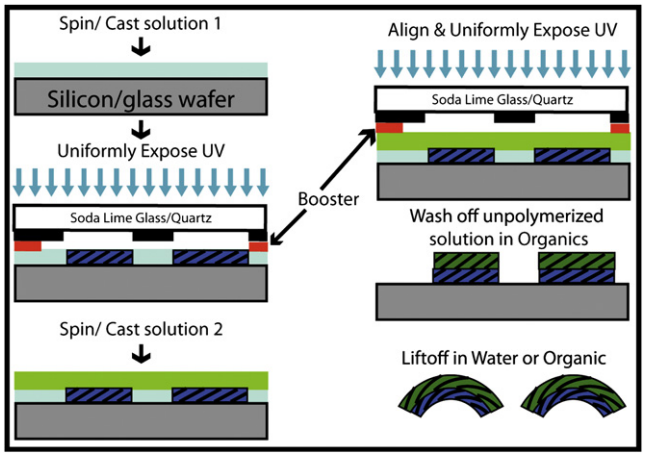

Fig. 1. Process flow for lithographic fabrication of bilayer structures. The PEODA/NIPAm-AAc bilayers were prepared by spin coating PEODA solution on a slide at 1000 rpm. After exposing at 50 mJ/cm^2 in non-contact mode, the second solution (NIPAm-AAc) was cast on top and exposed at 35 mJ/cm^2. The polymerized patterns were washed with ethanol and developed in their swollen state in ethanol.

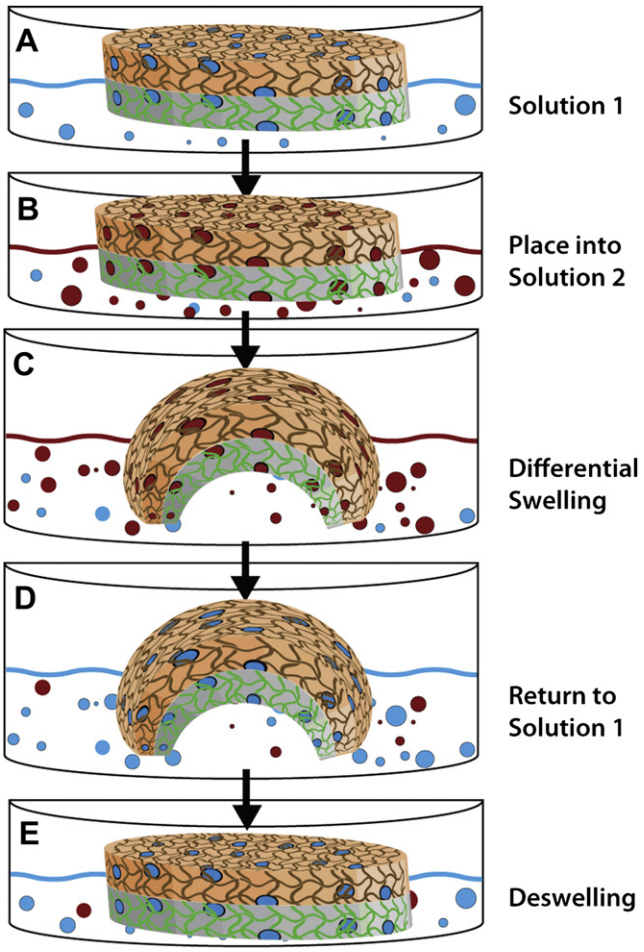

Fig. 2. Schematic of the bilayer actuation mechanism. A: A hydrogel bilayer is placed in aqueous solution 1 with specific pH and IS. It comes to equilibrium. B: The bilayer is transferred to solution 2 which has different pH and IS. C: Gel 1 swells in response to the environmental changes while Gel 2 does not swell, causing the bilayer to fold. D: The bilayer is transferred back into solution 1. E: Gel 1 deswells in response to the environmental changes and the bilayer unfolds.

equilibrate, and then placed in the solution in question. After equilibrating to the pH/IS for 7 h, the gels were weighed, left to dry over three days, and weighed again. For each sample, all stages of weighing were accomplished in the same centrifuge tube to minimize handling. Weights were recorded as weight of wet or dry gel plus tube, and all tubes were weighed prior to the experiment. The average swelling ratio and standard deviation were computed from three samples placed in same pH and IS (Table 1). The swelling ratio was calculated as follows:

$$\text{Swelling Ratio} = \frac{W_S - W_D}{W_D} \times 100 \quad (1)$$

W_s :Weight of Swollen Gel; W_D :Weight of Dry Gel.

3. Results and discussion

3.1. Effect of IS and pH on swelling

Swelling ratio tests revealed differing swelling behaviors for the polymerized gels, with data shown in Table 1. The average swelling ratio was plotted against pH at constant IS and against IS at constant pH as shown in Fig. 3. pH-sensitive hydrogels swell or contract in response to pH changes as a result of the charge density of the material. Acidic hydrogels, such as NIPAm-AAc, swell in solutions with a pH above the pKa of the hydrogel [19] due to the ionization and subsequent dissociation of the acid groups in the hydrogel. As governed by the Donnan equilibrium, an osmotic pressure proportional to the difference in mobile ion concentration between the inside and outside of the hydrogel is generated [20,21]. Changes in IS alter the Debye screening lengths of hydrogels [22], causing swelling or contraction due to different degrees of self-repulsion of the hydrogel monomers. Specifically, increasing the concentration of salt in solution causes the mobile ion concentration outside of the hydrogel to approach or even surpass the mobile ion concentration within the hydrogel. This change in the osmotic pressure causes reduced swelling in ionized hydrogels or de-swelling in neutral hydrogels [23]. The maximum swelling is constrained by the cross-linking of the chains [24]. The transport and diffusion of ions through hydrogels and the resultant kinetics of swelling are complex and explored elsewhere [24–26].

At low IS, NIPAm gels started to show an increase in swelling at low pH, however a sharp decrease was observed at high pH conditions. This declining behavior was fairly similar for the various IS conditions. NIPAm gels were relatively sensitive to changes in IS, with average swelling ratios exhibiting a decreasing trend from 1000 at 0.2M to 450 at 1.1M.

When copolymerized with AAc, we observed a higher swelling ratio across all pH and IS levels, and a greater sensitivity of the gels to pH changes at the low end (2.5 and 4.8). NIPAm-AAc demonstrated

Table 1
Hydrogel swelling data. Recorded swelling ratios for patterned polymers used in this study. SD = Standard Deviation of 3 samples.

pH	Ionic Strength (M)	NIPAm		NIPAm-AAc		NIPAm-HEMA		PEODA	
		Swelling Ratio	SD	Swelling Ratio	SD	Swelling Ratio	SD	Swelling Ratio	SD
2.5	0.2	1086.1	47.4	1058.3	123.3	521.4	96.1	143.3	82.0
	0.5	837.5	114.3	635.7	129.2	543.5	91.6	222.0	171.4
	0.8	511.6	86.3	591.7	76.4	662.6	23.1	141.5	52.2
	1.1	331.5	29.0	298.3	77.5	487.0	50.7	91.1	12.5
4.8	0.2	1307.2	149.7	1390.0	130.8	628.0	71.3	175.8	49.7
	0.5	885.6	162.1	1031.7	33.4	514.2	178.6	90.3	25.4
	0.8	538.3	122.1	749.2	118.0	605.6	26.8	416.1	202.8
	1.1	476.2	48.3	425.0	58.3	504.6	88.6	174.9	136.9
7.8	0.2	782.2	107.8	1505.6	162.8	688.9	76.2	120.4	20.5
	0.5	876.7	125.0	1103.1	34.5	581.9	60.7	177.9	69.1
	0.8	399.4	35.4	828.2	87.5	553.5	42.2	247.0	137.7
	1.1	476.7	87.4	771.4	67.2	545.0	82.6	151.8	61.4
12.1	0.2	470.6	50.9	1233.4	60.8	501.6	32.3	131.1	13.5
	0.5	444.4	58.5	827.9	113.2	547.2	91.9	264.1	58.7
	0.8	409.8	39.1	688.9	50.9	490.7	34.1	216.7	125.2
	1.1	390.3	78.2	646.1	19.8	497.9	65.6	285.3	39.7

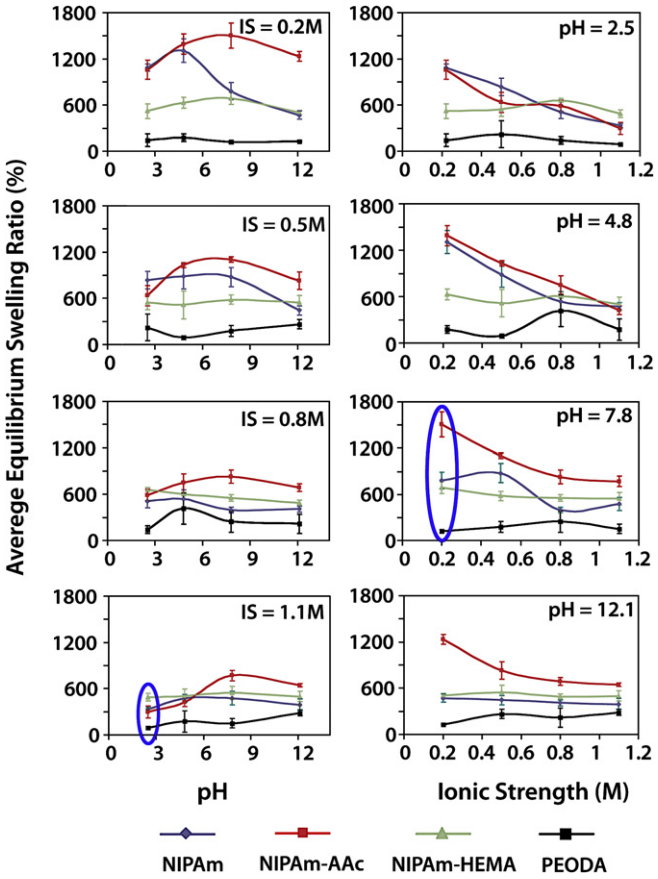

Fig. 3. Swelling characteristics of patterned hydrogels. NIPAm and NIPAm-AAc gels exhibited a general trend in which the average swelling ratio declined with an increase in IS. The average swelling ratio for NIPAm-AAc gels showed a bell like curve for several pH conditions. We observed a peak in swelling at pH 7.8 for the four plots. However, as the IS increased, the average swelling peak decreased from 1505 to 771. 50% shrinkage for NIPAm-AAc was achieved at pH 7.8 by changing IS alone. PEODA gels exhibited the least amount of swelling in all pH and IS solutions.

a bell like curve for the average swelling ratio when exposed to several pH conditions. We observed a peak in swelling at pH 7.8 for the four swelling ratio v. IS plots in Fig. 3. However as the IS of the solution increased, the average swelling ratio decreased from 1505 to 771 as shown in Table 1. A 50% shrinkage was readily achieved at a single pH condition (7.8) with increasing IS.

For copolymerized HEMA and NIPAm in a DMSO solvent, we observed insensitivity in swelling of the gels, which showed an average swelling ratio of 500–700 regardless of aqueous conditions tested. As expected, the PEODA was also relatively less sensitive to the solution pH and IS. Almost all combinations (of the 16 tested) resulted in swelling of 100–300%. We also observed that all NIPAm derivatives experienced swelling in organic solvents such as ethanol, while PEODA showed minimal swelling.

Overall, NIPAm-AAc showed the most sensitivity to changes in pH due to the dissociation of its acid groups [20,21]. PEODA and HEMA were mostly insensitive to pH. All of the hydrogels showed some sensitivity to IS, specifically showing a decrease in swelling with increasing IS. This can be attributed to the similarity of mobile ion concentration inside and outside of the hydrogels [23].

3.2. Bilayer patterning and folding

To create stimuli-responsive folding bilayers, two hydrogels were patterned in sequence. The layers were chosen to maximize the swelling differential along their common boundary; one layer should swell in response to changes in pH and IS, while the other should remain static. This would induce stress at their common boundary, causing the bilayer to fold.

Bilayers of NIPAm-AAc and PEODA were fabricated to test their ability as an all-polymer actuator. A comparison of NIPAm-AAc swelling to that of PEODA in solutions of different IS and pH showed vast differences in the two layers' swelling properties. As NIPAm-AAc was transferred from a pH 2.5/IS 1.1M solution to a pH 7.8/IS 0.2M solution, its swelling ratio increased from ~300 to ~1500. However, the PEODA swelling ratio only increased from 91 to 120. This difference suggested that bilayers of the two would fold due to the high differential swelling of the two hydrogel layers.

Individual layers of NIPAm-AAc and PEODA adhered to each other well and no delamination was observed (Fig. 4). Patterned

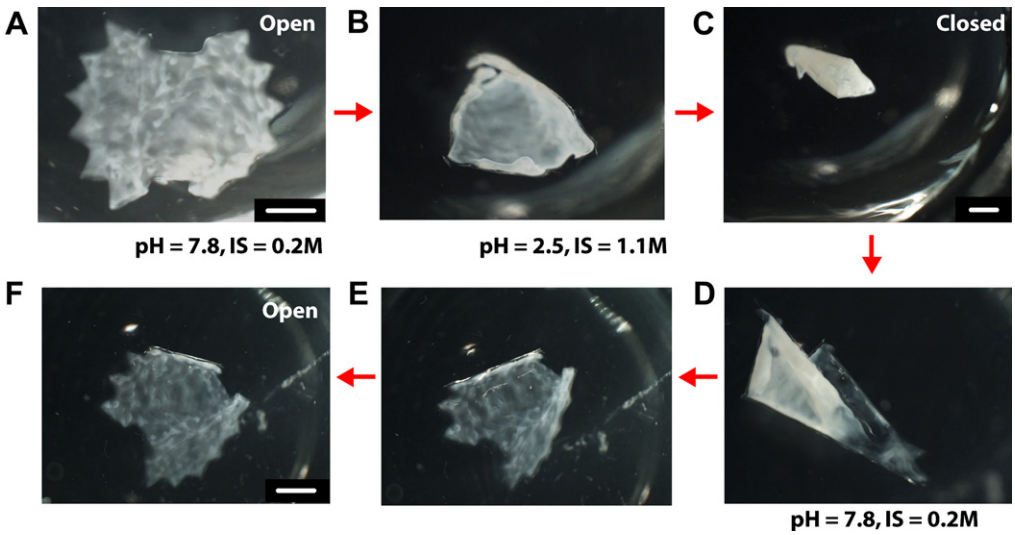

Fig. 4. All-hydrogel bilayer folding and unfolding. Reversible folding was achieved by first exposing the bilayer gel to a solution of pH 7.8 at IS 0.2M. Panels B–C show folding behavior of this bilayer structure after introducing a pH 2.5/1.1 M IS solution. Once complete folding was achieved in panel C, the original solution (pH 7.8/0.2 M IS) was introduced to achieve maximum swelling and thus unfolding of the bilayer as shown in panel F. The folding occurred over several minutes, and were repeated over 5 cycles. Scale bars are 1 mm.

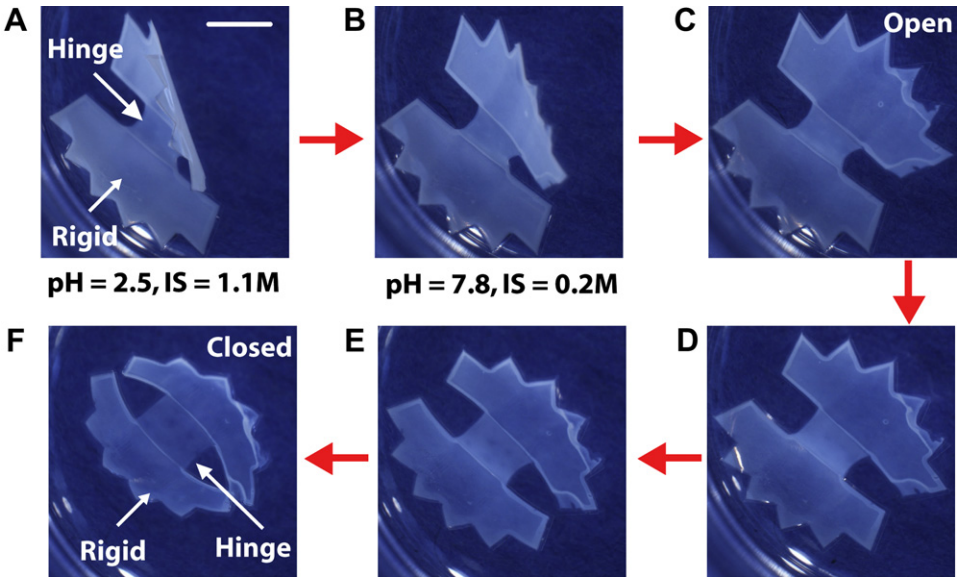

Fig. 5. Actuator with hinges folding in changing pH/IS.VF-shaped actuator constructed from rigid SU-8 segments with a NIPAm-AAc/PEODA bilayer hinge. Reversible folding occurred when the structure was transferred from a pH 2.5/IS 1.1 M solution to a pH 7.8/IS 0.2 M solution. The folding was reversible over 15 cycles. Scale bar is 3 mm.

bilayers were released from the glass substrate by immersion in ethanol and water. A primary challenge during photopatterning was registration of multiple layers of transparent polymers. However, during development it was possible to check registration of the bilayers as the NIPAm-AAc was transparent and PEODA is translucent as patterned. It was also possible to use metallic alignment marks on the glass surface to aid in registration.

Initially in a pH 7.8/IS 0.2M solution, a PEODA/NIPAm-AAc bilayer was at equilibrium with no stress across the interface. As it was transferred to a pH 2.5/IS 1.1M solution, the NIPAm-AAc layer contracted by a factor of 4, causing a compressive stress and folding the bilayer. The stress was channeled by the VF pattern, and the entire bilayer folded over several minutes, as seen in Fig. 4. When returned to the original solution, the bilayer unfolded into its initial state. The hydrogel bilayers were reversible over five cycles in the two solutions.

Of relevance to biological applications, we note that the materials themselves are known to be biocompatible. Additionally, the molecular structures of the hydrogels can be tuned and the resulting pH and IS thresholds can be varied for specific applications. In the current system, although an actuation pH of 2.5 may seem low, these pH values are encountered in the stomach (pH can be as low as 1). Additionally, while mammalian cells cannot survive for extended periods at high osmolarity, the range we used is within limits for many medical encounters such as infusions for parenteral nutrition [27], gastric and small intestine fluids [28], and urine [29].

3.3. *Venus flytrap patterning and folding*

Hinged structures in the shape of a VF were fabricated with rigid SU-8 panels and PEODA/NIPAm-AAC bilayer hinges. SU-8 was chosen for the rigid segments because it is structurally rigid and biocompatible. Additionally, it is highly crosslinked and chemically-resistive; for example, it swells only 0.5% in Dulbecco's phosphate buffered saline [30]. The bilayer polymers adhered well to atmospheric plasma-treated SU-8 and to each other. The structures released easily from the glass substrate in water. Registration of the layers was made easier because of the opacity of the SU-8 panels.

The hinged VF shapes have a different equilibrium state than the bilayer structures due to the difference to initial stress created in the hinge bilayer from patterning over the uneven geometry of the SU-8 rigid panels. Their initial state in a pH 7.8/IS 0.2M was folded to a higher angle (as compared to bilayer folding) due to significant NIPAm-AAc swelling. When transferred to a pH 2.5/IS 1.1M solution, the NIPAm-AAc layer contracted, generating compressive stress, causing the structure to unfold and then fold in the same direction as the bilayer folding, as seen in Fig. 5.

The rigid SU-8 panels maintained the structure of the VF shape and only folded along the bilayer hinge, whereas bilayer shapes actuated along the entire surface, causing a rolling effect. The folding action took place in anywhere from 10 s to several minutes, depending on the thickness of the hinge layers. The VF's were reversible over 15 cycles.

4. Conclusion

We have demonstrated an integrated approach to create hydrogel bilayers via lithographic patterning that fold and unfold in response to changing aqueous conditions. By choosing patternable acrylate derivatives such as PEODA and NIPAm-AAc, regions with high differential swelling characteristics were created.

We analyzed the swelling ratios for the chosen polymers in a variety of pH and IS conditions, and then constructed a patterned bilayer that folded in the expected manner. This bilayer closed and re-opened using the energy of the solution, without wires or electricity. We also constructed VF-shaped hinged structures with SU-8 rigid panels and a hydrogel bilayer hinge which folded in response to changes in IS and pH.

A highlight of this technique is the ease by which a stimuli-responsive polymer can be turned into an actuator. The ease and simplicity of this parallel fabrication scheme makes this technology accessible and highly economical. While our actuator operated on the time scale of minutes, we expect that actuation time will decrease as a function of further miniaturization [25,31].

By utilizing biocompatible polymers and hydrogels, these actuators have potential across the biological and medical fields in the areas of drug delivery and implantable tools. The combination of patterned all-polymer rigid panels and flexible hydrogel hinges allows for a wide variety of geometries. Different combinations of flexible hinges and rigid segments should yield cylinders, spirals, and

other highly-defined conformations [32]. Such structures may have distinct advantages in the area of 3D cell culture or reconfigurable microfluidics. Reversibility of these bilayer actuators is advantageous for these applications, allowing for repeated sensing, mixing, or sampling in response to continuous environmental change. For example, the ability to actuate around cells that could later be released easily for analysis with minimal damage would be ideal for sampling. Alternately, it would allow for loading of cargo in the folded state and subsequent release of cargo as the actuator opens.

We anticipate that this approach will allow the utility of photolithographic patterning of polymers to be explored for utilization in self-assembly. While rigid components may be used as side walls or tool bits, active hinge elements can be developed for the specific environment by selecting appropriate polymer combinations. The creation of such bio-friendly, all-polymeric, self-assembling devices would have applications in the biological and medical fields, especially in the areas of 3D cell culture, drug delivery, and non-invasive microsurgery.

Acknowledgment

The authors acknowledge funding support from the Beckman Foundation and the Camille and Henry Dreyfus Foundation, and the Northrop Grumman Fellowship at the Institute for Nano-BioTechnology at JHU. The authors thank Alla Brafman for useful discussions.

References

[1] Jackman RJ, Brittain ST, Adams A, Wu H, Prentiss MG, Whitesides S, et al. Langmuir 1999;15(3):826–36.
[2] Leong TG, Benson BR, Call EK, Gracias DH. Small 2008;4(10):1605–9.
[3] Leong TG, Lester PA, Koh TL, Call EK, Gracias DH. Langmuir 2007;23(17):8747–51.
[4] Leong TG, Randall CL, Benson BR, Bassik N, Stern GM, Gracias DH. Proceedings of the National Academy of Sciences 2009;106(3):703–708.
[5] Randhawa JS, Leong TG, Bassik N, Benson BR, Jochmans MT, Gracias DH. Journal of the American Chemical Society 2008;130(51):17238–9.
[6] Leong TG, Zarafshar AM, Gracias DH. Small 2010;6(7):792–806.
[7] Prinz VY, Seleznev VA, Gutakovsky AK, Chehovskiy AV, Preobrazhenskii VV, Putyato MA, et al. Physica E: Low-dimensional Systems and Nanostructures 2000;6(1–4):828–31.
[8] Smela E, Inganas O, Lundstrom I. Science 1995;268:1923–9.
[9] Guan J, He H, Hansford DJ, Lee LJ. The Journal of Physical Chemistry B 2005;109(49):23134–7.
[10] He HY, Guan JJ, Lee JL. Journal of Controlled Release 2006;110(2):339–46.
[11] Kelby TS, Huck WTS. Macromolecules 2010;43(12):5382–6.
[12] Yu L, Urban G, Moser I, Jobst G, Gruber H. Polymer Bulletin 1995;35(6):759–65.
[13] Duracher D, Sauzedde F, Elaissari A, Perrin A, Pichot C. Colloid & Polymer Science 1998;276(3):219–31.
[14] Duracher D, Sauzedde F, Elaïssari A, Pichot C, Nabzar L. Colloid & Polymer Science 1998;276(10):920–9.
[15] Snowden MJ, Chowdhry BZ, Vincent B, Morris GE. Journal of the Chemical Society, Faraday Transactions 1996;92(24):5013–6.
[16] Szczubiałka K, Moczek I, Błaszkiewicz S, Nowakowska M. Journal of Polymer Science Part A: Polymer Chemistry 2004;42(15):3879–86.
[17] Bassik N, Abebe BT, Gracias DH. Langmuir 2008;24(21):12158–63.
[18] Forterre Y, Skotheim JM, Dumais J, Mahadevan L. Nature 2005;433(7024):421–5.
[19] Peppas NA, Khare AR. Advanced Drug Delivery Reviews 1993;11(1–2):1–35.
[20] Ahn S-k, Kasi RM, Kim S-C, Sharma N, Zhou Y. Soft Matter 2008;4(6):1151–7.
[21] Somasundaran P. Encyclopedia of surface and colloid science, vol. 5. Boca Raton: CRC Press; 2006.
[22] Kratz K, Hellweg T, Eimer W. Colloids and Surfaces A: Physicochemical and Engineering Aspects 2000;170(2–3):137–49.
[23] Liu X, Tong Z, Hu O. Macromolecules 1995;28(11):3813–7.
[24] Peppas NA, Huang Y, Morres-Lugo M, Ward JH, Zhang J. Annual Review of Biomedical Engineering 2000;2:9–29.
[25] Amsden B. Macromolecules 1998;31(23):8382–95.
[26] Masaro L, Zhu XX. Progress in Polymer Science 1999;24(5):731–75.
[27] Gura KM. Nutrition in Clinical Practice 2009;24(6):709–17.
[28] Fordtran J, Locklear T. Digestive Diseases and Sciences 1966;11(7):503–21.
[29] Dugdale DCI. Oslmolarity - Urine. MedlinePlus, vol. 2010. U.S. National Institutes of Health; 2009.
[30] Chronis N, Lee LP. Journal of Microelectromechanical Systems 2005;14(4):857–63.
[31] van der Linden HJ, Herber S, Olthuis W, Bergveld P. The Analyst 2003;128(4):325–31.
[32] Bassik N, Stern GM, Jamal M, Gracias DH. Advanced Materials 2008;20(24):4760–4.